Spin correlation studies of FeF$_2$ and Fe$_{0.6}$Zn$_{0.4}$F$_2$ by optical exciton-magnon transitions

Spin correlation studies of FeF_2 and $Fe_{0.6}Zn_{0.4}F_2$ by optical exciton–magnon transitions

W Kleemann and R Uhlig

Angewandte Physik, Universität Duisburg, D-4100 Duisburg 1,
Federal Republic of Germany

Abstract. The fine structure and the temperature dependence of the moments M_0, M_1 and M_2 of a sharp and isolated exciton–magnon absorption line near $\lambda = 465$ nm are studied on FeF_2 and $Fe_{0.6}Zn_{0.4}F_2$. The results compare well with theoretical predictions of Tanabe and co-workers, since overlap with other magnon or phonon sidebands is nearly negligible. *All* moments show cusp-like behaviour at T_N owing to singularities of the spin correlation functions involved. In $Fe_{0.6}Zn_{0.4}F_2$ additional precursor peaks arise at $T \simeq 1.2\ T_N$. They are attributed to enhanced short-range order characteristic of reduced dimensionality.

1. Introduction

Since the pioneering experimental work of Sell *et al* (1967) and the complementary theory of Shinagawa and Tanabe (1971) and Fujiwara and Tanabe (1972) optical exciton–magnon transitions have been considered well established tools for studying spin correlations at magnetic phase transitions of insulating crystals. However, quantitative agreement between experimental data of the moments, M_0, M_1 and M_2 versus T (see e.g. Fujiwara *et al* 1972), and theoretical predictions has rarely been achieved. This is primarily due to unavoidable superpositions of the exciton–magnon absorption with exciton–phonon and exciton–magnon–phonon processes. This may explain why many authors confine themselves to explaining their results by mean-field arguments (Yen *et al* 1967) rather than applying the more elaborate microscopic theory.

For example, recently the blue shifts of broad exciton bands were related to $\langle S_z \rangle^2$ in MnO (Seehra and Groves 1983) and to $\langle S_z \rangle$ in MnF_2 (Seehra and Abumansoor 1985), where $\langle S_z \rangle$ is the sublattice magnetisation. However, in order to understand non-vanishing contributions *above* the Néel temperature, T_N, proportionality with the magnetic energy, $\langle S_i \cdot S_j \rangle$ had to be invoked. Clearly, neither $\langle S_z \rangle^2$ nor $\langle S_z \rangle$ nor $\langle S_i \cdot S_j \rangle$ do fully account for the microscopic mechanisms (Fujiwara and Tanabe 1972). These involve non-negligible contributions of three- and four-spin correlation functions to the transition moments in addition to those of two-spin correlations.

In this paper we consider the well known three-dimensional (3d) Ising antiferromagnet FeF_2 as an almost ideal candidate for quantitative comparison of exciton–magnon absorption with theory. Hitherto only low-temperature studies have been done on some magnon sidebands of this system. They refer to crystal-field transitions (Kambara 1968) in the near infrared (Tylicki and Yen 1968) and in the 385–465 nm

spectral region (Chen *et al* 1971). In the latter range we selected one particularly sharp and well resolved exciton–magnon line at 465 nm, which is very suitable for studying temperature dependences up to room temperature. Many features predicted theoretically could be confirmed in a particularly clear manner.

Encouraged by the clarity of the results obtained on FeF_2 we also studied the dilute system $Fe_{0.6}Zn_{0.4}F_2$, which is known as a prototype random-exchange Ising model system (Birgeneau *et al* 1983). Effects of randomness are expected to modify not only the critical behaviour, but also the non-critical spin correlations, which are relevant to the *T*-dependence of the moments.

2. Experimental procedure and results

The samples of FeF_2 and $Fe_{0.6}Zn_{0.4}F_2$ were cut parallel to the {100} faces of Bridgman-grown single crystals (N Nighman, Physics Department, University of California at Santa Barbara). They had typical edge lengths of 2–3 mm. Temperatures between 12 and 300 K, stabilised to better than 0.1 K, were achieved using a closed-cycle refrigerator cryostat (Leybold ROK 10-300). Unpolarised axial absorption spectra were measured with a computerised Cary 14 spectrophotometer at wavelengths between 350 and 600 nm with a resolution of better than 0.1 nm using digitisation steps of 0.01 nm. Values obtained at $T = 12$ K are shown in figure 1(*a*) for FeF_2 and figure 1(*b*) for $Fe_{0.6}Zn_{0.4}F_2$. Broad bands and groups of narrow lines are observed. They correspond to the transitions within the d^6 electronic configuration of the Fe^{2+} ions in a cubic crystal field with $Dq/B = 0.8$ (Kambara 1968). In figure 1 they are labelled C to H in order of increasing energy. A and B refer to wavelengths $\lambda > 600$ nm (Tylicki and Yen 1968) and are not shown.

The E lines in both figure 1(*a*) and (*b*) are particularly strong and sharp. As discussed by Chen *et al* (1971), they refer to one of the transitions $^5T_{2g} \rightarrow {}^3E_g$ or $^3T_{1g}$. At low temperatures a subtle fine structure is resolved in the case of pure FeF_2 (figure 2(*a*)). Apart from the prominent one-magnon cold band M^+ at 463.7 nm (21 566 cm^{-1}) one observes the weak lines Ex at 465.0 nm (21 507 cm^{-1}) and $2M^+$ at 462.4 nm (21 628 cm^{-1}), corresponding to the pure exciton and to the two-magnon cold band, respectively. A one-magnon hot band, M^-, emerges at 466.8 nm (21 422 cm^{-1}) on increasing *T*. As usual (Meltzer *et al* 1969) it lies more distant from the electronic origin, Ex, than does the cold band, M^+. With increasing temperature the line Ex vanishes and the M^+ line broadens and shifts towards lower energies. At temperatures above $T_N = 78.3$ K, M^+ and M^- merge into one another, the centre of gravity ($=M_1$) shifts from the cold- to the hot-band side and fine structure becomes smeared out. Different pair processes are ill defined at $T > T_N/3$, say (Fujiwara *et al* 1972). That is why only the method of moments makes sense in the evaluation of the data in the total regime of temperatures (see below). Appropriate theoretical predictions are lacking for the *T*-dependences of single lines (M^+, Ex, M^-), whose discrete evaluation might look tempting in the low-*T* limit.

Dilution of FeF_2 with ZnF_2 by a molar fraction of $x = 0.4$ causes a red shift of the M^+ line of merely 1.65 nm, but a considerable broadening of its low-*T* FWHM from 0.6 to 2.7 nm (figure 2(*a*) and (*b*)). Hence, even at low temperatures any fine structure is smeared out. It should be stressed that the broadening is not due to concentration gradients. Since the position of the M^+ line depends only weakly on *x* (see above), which varies by no more than $\Delta x = \pm 0.01$ in our sample (Birgeneau *et al* 1983), line broadening
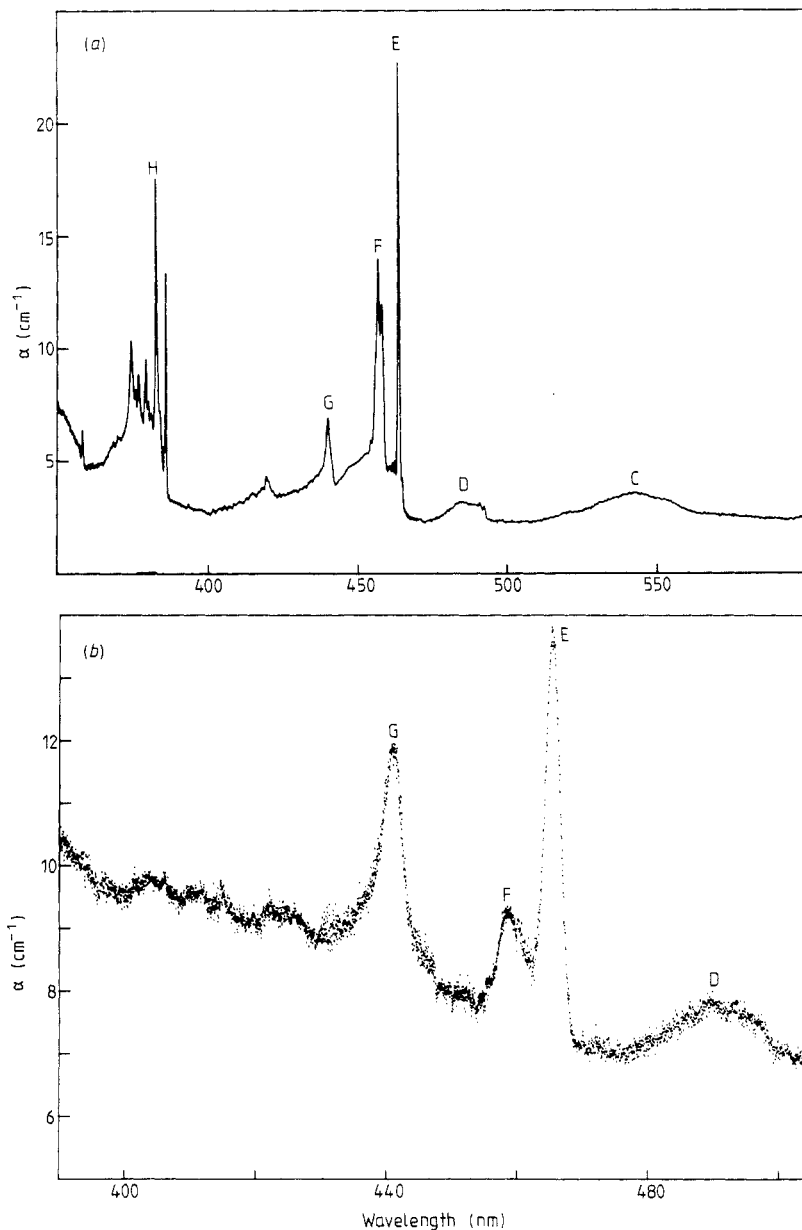
Figure 1. Axial absorption spectra of FeF$_2$ (a) and Fe$_{0.6}$Zn$_{0.4}$F$_2$ (b) measured at $T = 12$ K. The labels C to H correspond to crystal-field states at increasing energy (see text).

due to Δx is expected to be smaller than 0.1 nm. We rather assume inhomogeneous broadening due to the microscopic variations of x, giving rise to large local crystal-field fluctuations. Again, a low-energy shift of the absorption line towards the hot-band side is observed as T is increased above $T_N = 49$ K (Birgeneau *et al* 1983). The approximate position of M$^-$ ($\approx$467.75 nm, arrow in figure 2(b)) is estimated from the corresponding energy difference $\delta E = E(\mathrm{M}^+) - E(\mathrm{M}^-)$ of pure FeF$_2$ (figure 2(a)) by assuming proportionality of δE with T_N.
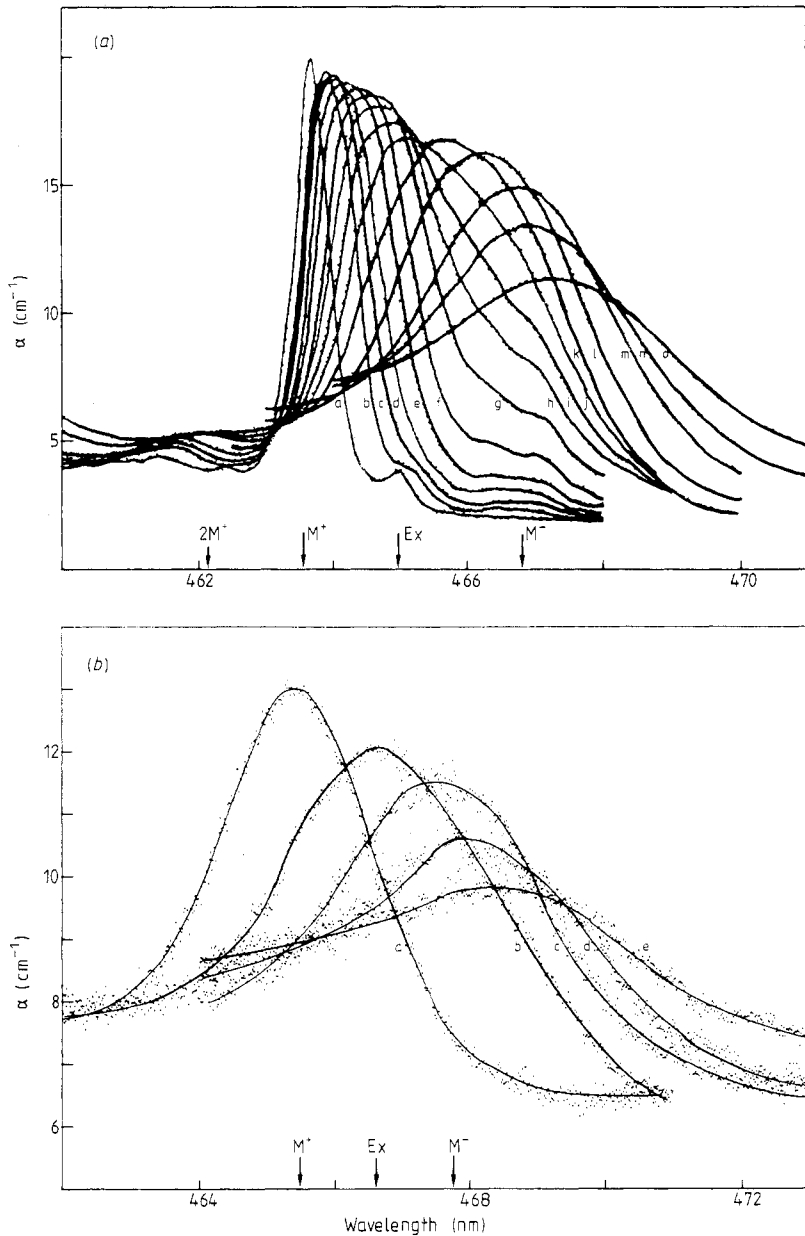
Figure 2. Axial E absorption (see figure 1) measured on FeF_2 (a) at $T = 12$ (a), 40 (b), 46 (c), 52 (d), 57 (e), 63 (f), 69 (g), 73 (h), 75 (i), 77 (j), 80 (k), 104 (l), 173 (m), 223 (n) and 293 K (o), and on $Fe_{0.3}Zn_{0.4}F_2$ (b) at $T = 12$ (a), 49 (b), 120 (c), 200 (d) and 293 K (e), respectively. The positions of the lines Ex, M^-, M^+, $2M^+$ (see text) are indicated by arrows.

The temperature dependences of the moments M_0, M_1 and M_2 of the absorption lines are shown in figures 3–5. They refer to about 70 spectra, some of which are shown in figure 2. The absorption intensities $M_0 = \int \alpha(\lambda) \, d\lambda$ versus T, as presented in figure 3 are roughly corrected by assuming linear background absorption, interpolating between the reference points $\lambda = 460$ and 475 nm. M_0 versus T of FeF_2 shows a cusp-like sharp
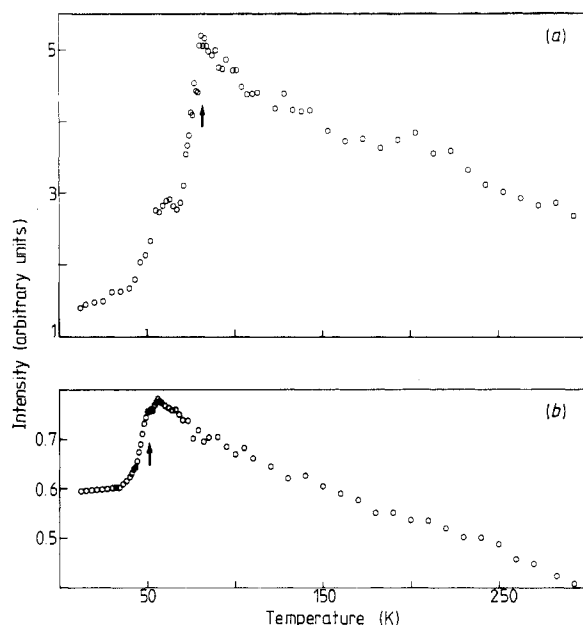
Figure 3. Temperature dependence of the integrated axial E absorption intensity (see figure 2) of FeF$_2$ (a) and Fe$_{0.6}$Zn$_{0.4}$F$_2$ (b). The cusps at T_N are indicated by arrows.

peak at about 80 K $\simeq T_N$, similarly as predicted by Shinagawa and Tanabe (1971), but much clearer than observed on MnF$_2$ or RbMnF$_3$ (Fujiwara *et al* 1972). We find an enhancement of M_0 by 400% between $T = 0$ and T_N, by far exceeding the 25% effect observed on the Mn^{2+} salts. Beyond the cusp, at $T > T_N$, M_0 decreases smoothly until reaching a value of about $2M_0(0)$ at room temperature.

In the diluted system, Fe$_{0.6}$Zn$_{0.4}$F$_2$, the absorption intensity increases by only 25% at temperatures up to T_N, which is indicated by a kink-like smeared cusp. Most remarkably, however, M_0 grows by another 5% on heating and peaks at about 60 K, before decreasing smoothly at increasing T. A similar precursor peak at about 60 K arises in the second moment, M_2 versus T, of Fe$_{0.6}$Zn$_{0.4}$F$_2$. This is shown by spectral half-width (FWHM) data in figure 4(b). For the pure compound, again, we merely find a cusp peaking exactly at T_N (figure 4(a)), similarly as reported for MnF$_2$ (Seehra and Abumansoor 1985). It should be noted, however, that the total increase of M_2 between $T = 0$ and T_N is much smaller in MnF$_2$ ($\sim$100%) than in FeF$_2$ ($\sim$600%). An even smaller rate (55%) is observed on Fe$_{0.6}$Zn$_{0.4}$F$_2$.

The first moments, M_1 versus T, are presented in figure 5 by the blue shifts of the centres of gravity of the exciton–magnon band upon cooling. $T = 293$ K is chosen as a reference temperature. At low temperatures the blue shift is roughly proportional to the magnetic energy, which may be obtained, for example, from magnetic linear birefringence data (Jahn 1973). Both M_1 and Δn versus T exhibit points of inflexion at T_N. At closer inspection of figure 5(a) and (b), however, one detects weak superimposed cusps peaking downwards at T_N. Hence, in the critical region the derivatives, dM_1/dT versus T are *not* proportional to the specific heat, c_m versus T, in contrast with the T-dependence of dΔn/dT (Belanger *et al* 1983).

It is interesting to note that the line positions at the Néel point, $M_1(T_N)$ (see curves 10 and 2 in figures 2(a) and (b), respectively), nearly coincide with the orbital excitation energies, $E(Ex)$, in agreement with a prediction of Tanaka (1971). Closer inspection, however, reveals that the blue shift of FeF_2, $\delta_1 = M_1(T_N) - M_1(0) = 77$ cm^{-1}, is larger than the low-T line separation, $\delta_2 = E(M^+) - E(Ex) = 59$ cm^{-1}. Remarkably, δ_1 is exactly the zone-edge magnon energy (Fleury *et al* 1966), whereas δ_2 appears reduced by exciton–magnon interaction (Chen *et al* 1971). In $Fe_{0.6}Zn_{0.4}F_2$, $\delta_1 = 59$ cm^{-1} is smaller than in the pure compound, albeit larger than expected from a simple proportionality with T_N or with the $T = 0$ exchange field, respectively (Yen *et al* 1967).

The concave T-dependence of M_1 within $T_N \lesssim T \lesssim 1.5\, T_N$ corresponds to that observed in Δn versus T and is due to short-range spin correlations. At $T \gtrsim 1.5\, T_N$, M_1 varies approximately linearly with T. We believe this to be due to effects of the thermal lattice expansion. A full account of the magnetically induced blue shift will need, hence, careful correction for this background effect.

3. Discussion

At low temperatures, $T \lesssim T_N/2$, all of the moments, M_0, M_1 and M_2, vary approximately like the magnetic energy. Indeed, pair correlation terms proportional to inter-sublattice spin functions $\langle S_j \cdot S_i \rangle$ were shown (Fujiwara and Tanabe 1972) to dominate as $T \rightarrow 0$. Hence, within spin-wave approximation T^3 behaviour is expected. This is roughly confirmed by our data. After subtraction of the respective $T = 0$ values we find T^y-laws with $y = 4.2$ (1.6), 2.9 (1.6) and 2.3 (0.8) for M_0, M_1 and M_2 versus T of FeF_2 and $Fe_{0.6}Zn_{0.4}F_2$ (values in brackets). Experimental data up to $T < 2T_N/3$ were considered in the best-fit procedures. The flat behaviour ($y \simeq 1$) of the moments of the diluted system presumably reflects the inhomogeneous broadening, which determines quasi-invariability of the absorption line at low temperatures.

The total increase of both M_0 and M_2 within $0 < T < T_N$ (figures 3(a) and 4(a)) is much larger than in the isostructural compound MnF_2 (Fujiwara *et al* 1972, Seehra and Abumansoor 1985). As proposed by Fujiwara *et al* (1972) anomalously large hot-band contributions may be due to intra-sublattice exciton–magnon processes, which were neglected in the original theory (Shinagawa and Tanabe 1971). They are dominant for example in the case of the well known 427 nm line of $FeCl_2$ (Schnatterly and Fontana 1972, Robbins and Day 1976). In the low-T limit they vanish provided that the symmetry of the Néel ground state is given. This condition is not met in $Fe_{0.6}Zn_{0.4}F_2$ owing to its broken translational symmetry. This may explain the relatively small increase of both M_0 and M_2 within $0 < T < T_N$ in that case (figures 3(b) and 4(b)).

At high temperatures the absorption intensity is expected to approach the value $(S + 1)M(0)/3$ (Shinagawa and Tanabe 1971), hence $M_0(T = \infty) = M_0(0)$ for FeF_2 with $S = 2$. The continuous decrease of M_0 at $T > T_N$ may, indeed, be in favour of this prediction, although $M_0(293\text{ K}) \simeq 2M_0(0)$ is still far from the limiting value. Eventual deviations, if any, will be due to intra-sublattice contributions, which were neglected in the above extrapolation (Fujiwara *et al* 1972).

In the vicinity of T_N, M_0 is essentially determined by transverse two-spin correlation functions (Fujiwara and Tanabe 1972). They are predicted to vary approximately like the parallel susceptibility, $\chi_\parallel$ versus T, at $T > T_N$ and like the sublattice magnetisation, $\langle S_z \rangle$ versus T, at $T < T_N$. Indeed, the M_0 versus T data of FeF_2 (figure 3(a)) very closely resemble experimental data of $\chi_\parallel$ (Foner 1964) and $\langle S_z \rangle$ (Jaccarino 1965) within the
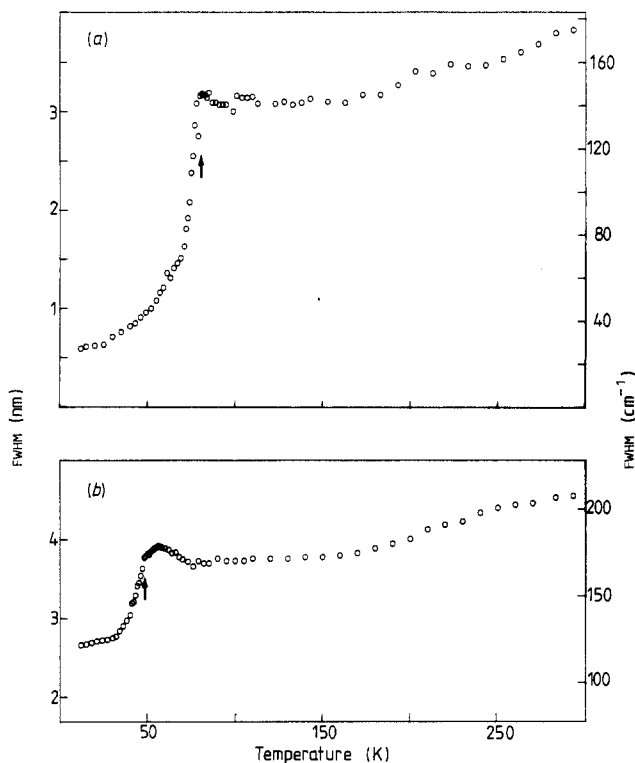
Figure 4. Temperature dependence of the full width at half maximum (FWHM) of the axial E absorption line (see figure 2) of FeF_2 (a) and $Fe_{0.6}Zn_{0.4}F_2$ (b). The cusps at T_N are indicated by arrows.

respective ranges of T. The cusp-like behaviour at T_N is, however, difficult to analyse, since various divergent spin correlation functions are superimposed and become relevant near T_N (Fujiwara and Tanabe 1972).

Very weak cusp-like behaviour of M_1 at T_N was predicted (Fujiwara and Tanabe 1972), but never observed experimentally. For the first time it is now verified by our present data on both FeF_2 and $Fe_{0.6}Zn_{0.4}F_2$ (figure 5, arrows). The observed small downward cusps are proportional to divergent spin correlation functions weighted by the difference ΔJ of the antiferromagnetic exchange constants in the ground and excited states involved in the optical transition. On the other hand very prominent cusp-like behaviour at T_N is expected to characterise M_2 versus T. It is determined by three- and four-spin correlation functions, all of which are predicted to maximise at T_N (Fujiwara and Tanabe 1972). The cusp found on FeF_2 is, indeed, quite distinct (figure 4(a)).

Most surprisingly, precursor fluctuation peaks at about $1.2T_N$ are characterising both M_0 and M_2 of diluted FeF_2. A similar feature remains unobserved in M_1 versus T, presumably since this is less sensitive to divergent spin correlations (see above). $Fe_{0.6}Zn_{0.4}F_2$ thus behaves like a low-dimensional system, where peaks of M_0 and M_2 are expected to arise at $T > T_N$ (Ebara and Tanabe 1974). Indeed, short-range order, which is typical of low-dimensional magnets, becomes increasingly important in diluted systems. As far as non-critical spin correlations are concerned their thermodynamical behaviour corresponds to reduced dimensionality (de Jongh 1983). At the percolation
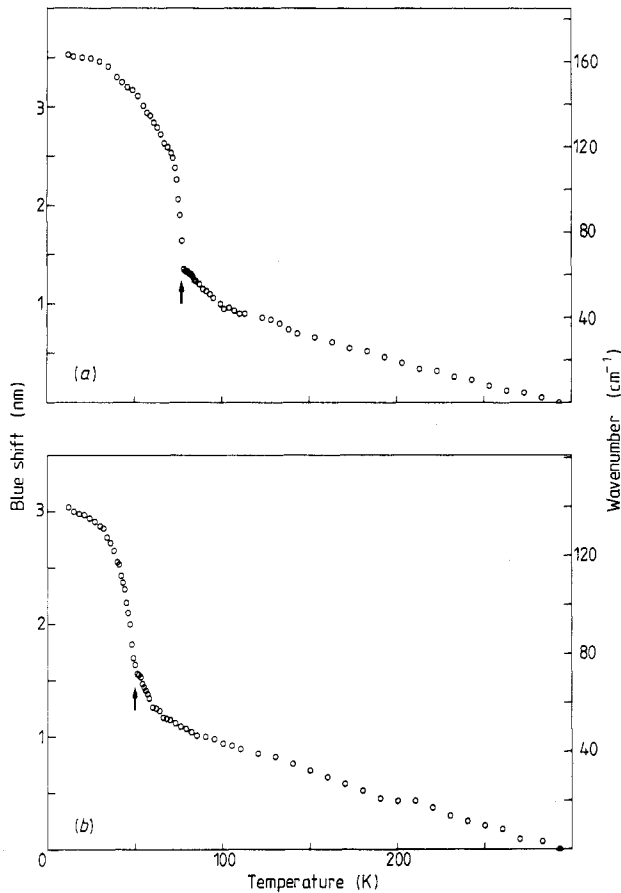
Figure 5. Temperature dependence of the blue shift with respect to the value at 293 K of the peak of the axial E absorption line (see figure 2) of FeF_2 (a) and $Fe_{0.6}Zn_{0.4}F_2$ (b). The cusps at T_N are indicated by arrows.

limit (about $Fe_{0.25}Zn_{0.75}F_2$) an effective dimension $d = 1$ is reached, where the residual cusps at T_N (figures 4(b) and 5(b), arrows) should eventually vanish. It will be interesting to study these novel effects systematically on various compositions of $Fe_xZn_{1-x}F_2$.

4. Conclusion

The magnon sidebands connected with the 465 nm exciton line in FeF_2 are particularly suited for studying the temperature dependences of exciton–magnon processes without serious perturbations by overlap with other phonon or magnon–phonon sidebands. For the first time contributions of transverse and longitudinal spin correlations, which maximise at T_N, are detected in *all* moments, M_0, M_1 and M_2. It would be worthwhile comparing the results with model calculations similarly as performed for MnF_2 (Fujiwara and Tanabe 1972). Higher resolution of the experimental data at $T \simeq T_N$ will be necessary for quantitative comparison. This applies in particular to the data of diluted samples,

$Fe_xZn_{1-x}F_2$ with $0.25 < x < 1$, where critical cusps and precursor short-range peaks appear superimposed.

Acknowledgments

References

Belanger D P, Nordblad P, King A R, Jaccarino V, Lundgren L and Beckman O 1983 *J. Magn. Magn. Mater.* **31–34** 1095–6

Birgeneau R J, Cowley R A, Shirane G, Yoshizawa H, Belanger D P, King A R and Jaccarino V 1983 *Phys. Rev.* B **27** 6747–53

Chen M Y, Scarpace F L, Passow M W and Yen W M 1971 *Phys. Rev.* B **4** 132–5

de Jongh L J 1983 *Magnetic Phase Transitions* ed. M Ausloos and R J Elliott (Berlin: Springer) pp 172–94

Ebara K and Tanabe Y 1974 *J. Phys. Soc. Japan* **36** 93–102

Fleury P A, Porto S P S, Cheesman L E and Guggenheim H J 1966 *Phys. Rev. Lett.* **17** 84–7

Foner S 1964 *Proc. Int. Conf. Magnetism (Nottingham)* (London: Inst. Phys. and Phys. Soc.) pp 438–42

Fujiwara T, Gebhardt W, Petanides K and Tanabe Y 1972 *J. Phys. Soc. Japan* **33** 39–48.

Fujiwara T and Tanabe Y 1972 *J. Phys. Soc. Japan* **32** 912–26

Jaccarino V 1965 *Magnetism* vol. 2a, ed. G T Rado and H Suhl (New York:Academic) p 328

Jahn I R 1973 *Phys. Status Solidi* b **57** 681–92

Kambara T 1968 *J. Phys. Soc. Japan* **24** 1242–64

Meltzer R S, Lowe M and McClure D S 1969 *Phys. Rev.* **180** 561–72

Robbins D J and Day P 1976 *J. Phys. C: Solid State Phys.* **9** 867–82

Schnatterly S E and Fontana M P 1972 *J. Physique* **33** 691–7

Seehra M S and Abumansoor S 1985 *Solid State Commun.* **56** 97–9

Seehra M S and Groves R D 1983 *J. Phys. C: Solid State Phys.* **16** L411–6

Sell D D, Greene R S and White R M 1967 *Phys. Rev.* **158** 489–510

Shinagawa K and Tanabe Y 1971 *J. Phys. Soc. Japan* **30** 1280–91

Tanaka H 1971 *J. Phys. Soc. Japan* **31** 368–77

Tylicki J and Yen W M 1968 *Phys. Rev.* **166** 488–94

Yen W M, Imbusch G F and Huber D L 1967 *Optical Properties of Ions in Crystals* ed. H M Crosswhite and H W Moos (New York: Interscience) p 301